Environment Parameter Estimation during Bilateral Telemanipulation*

Sarthak Misra
sarthak@jhu.edu

Allison M. Okamura
aokamura@jhu.edu

Department of Mechanical Engineering
The Johns Hopkins University
Baltimore, MD 21218, USA

ABSTRACT

Accurate models of remote environments generated during telemanipulation can be used to improve transparency, generate realistic simulations, and evaluate environment state. This paper presents an architecture for environment parameter estimation during bilateral telemanipulation. Nonlinear stiffness and damping properties of the environment are estimated using an indirect adaptive control approach. The slave-environment contact force tracks the sum of the force applied by the human to the master and a persistent excitation force required for accurate environment parameter estimation. Since force feedback to the human operator should only reflect the environment properties, several methods for force feedback are considered. Simulations confirm the validity of the proposed telemanipulation architecture for obtaining reasonable estimates of nonlinear environment properties and providing appropriate force feedback to the operator.

Keywords: telemanipulation, adaptive control, impedance control, environment stiffness and damping, force feedback

1 INTRODUCTION

A telemanipulator is an electro-mechanical system comprised of a master and a slave robot connected via a communication channel and controllers. The human operates a master device, while the slave robot directly interacts with the environment. To achieve reasonable performance in many telemanipulated tasks, the human operator needs information about the remote environment. Feedback can be provided in many different forms, including audio, visual, and haptic displays. The telemanipulated system is said to be bilateral if there is an exchange of energy between the master and slave robots through the feedback of force information [10].

This paper provides a method for extracting environment properties, specifically the stiffness and damping properties of soft materials, during bilateral telemanipulation. Bilateral telemanipulation is typically performed without explicit environment modeling. However, accurate models of remote environments generated during telemanipulation can be used to improve transparency, generate realistic simulations, and evaluate environment state. We are particularly interested in surgical robotics applications, where soft tissue models obtained during surgery may improve operator performance, develop realistic training systems, and enable online diagnosis. It is envisioned that, during tissue palpation, estimation of environment properties would help surgeons quantitatively track variations in stiffness and damping properties for diagnosis. Also, estimated environment properties would help in the development of realistic, patient-specific virtual environment models for surgical planning and training.

1.1 Previous Work

There are two main areas of prior work relevant to this research: soft tissue modeling and environment property estimation during telemanipulation.

Past research on soft tissue modeling has primarily focused on designing specialized surgical instruments and experimental apparatus for measuring tissue deformation and interaction forces, and using the resulting data to build finite element models, e.g. [1, 4, 13, 15, 24]. Most of this research uses phantom or *ex vivo* tissues, although *in vivo* tissues may have significantly different dynamics [18]. Researchers have also examined the theoretical and computational aspects of finite element modeling for soft tissues to be used in surgical simulators [3]. While the eventual goal of our work is to create similarly complex tissue models, in this paper we are concerned with the identification of the effective environment stiffness and damping parameters at a single location.

Environment property estimation has been performed by both autonomous and telemanipulated robots. Dupont, et al. [7] presented a high-level framework for property estimation during telemanipulation that considers three steps: task decomposition, data segmentation, and parameter estimation. Their algorithm directly computed the geometry, mass, and coefficient of friction of the environment, but did not generate sufficient excitation for estimation of damping. Park, et al. [19] presented a modified position-position telemanipulation architecture for online environment stiffness adaptation during force control of the slave robot. Hashtrudi-Zaad, et al. [11] presented simulation studies that achieved transparency during telemanipulation using a composite adaptive controller to estimate the dynamic properties of high-stiffness environments. Duchemin, et al. [6] used a hybrid force/position controller for robotic telesurgery in skin harvesting procedures. With appropriate choice of gains, their controller estimated skin stiffness, friction, and thickness. Diolaiti, et al. [5] and Colton, et al. [2], both used a least-squares method to estimate the stiffness of the environment. Alternatively, De Gersem, et al. [9] used a Kalman filtering technique to estimate the stiffness of soft materials during telemanipulation.

1.2 Contributions

The goal of this work is to estimate and collect environment properties during a telemanipulated procedure, while simultaneously providing the user with a realistic feel of the environment dynamics. The new contributions of this work include: (1) a computationally efficient and easily implementable online parameter estimation algorithm for bilateral telemanipulation systems, (2) estimation of both nonlinear stiffness and damping during telemanipulation, and (3) methods to prevent the excitation signals from being fed directly back to the human operator.
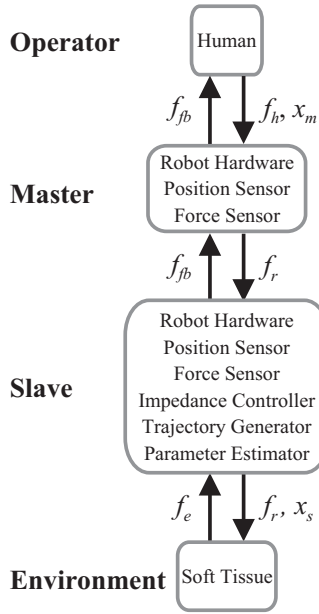
Figure 1: Bilateral telemanipulation system components for environment parameter estimation.

Figure 2: Complete control scheme for the bilateral telemanipulation system used for environment parameter estimation.

Environment parameter estimation is achieved by using an indirect adaptive control scheme [20]. The indirect adaptation law is formulated to ensure that the interaction force between the slave robot and its environment tracks the reference force provided from the master side. The indirect adaptive control approach has been considered because of its relative ease of implementation for real-time estimation of environment parameters [8].

This paper also addresses higher level questions associated with persistent excitation of the environment, which is required for good parameter estimation [23]. We consider a closed-loop telemanipulation system architecture, which includes the slave-environment interaction force fed back to the operator. Since the required excitation is oscillatory, the contact force is also time varying. Various force feedback methods are explored to cancel the oscillations and to give the operator a more "transparent" telemanipulation experience during the parameter estimation process.

2 INTEGRATING TELEMANIPULATION AND PARAMETER ESTIMATION

In this section, we present a bilateral telemanipulation architecture that includes an environment parameter estimation algorithm. Online parameter estimation using indirect adaptive control requires a trajectory generator and a parameter adaptation law. The online trajectory generator and indirect adaptive law enable force tracking between a reference force and the sensed slave-environment contact force. Richness of the reference force is required for the estimated environment parameters to converge to the actual values [23]. In the proposed telemanipulation system, the reference force is generated as the sum of the force applied by the human operator to the master robot and a high-frequency excitation force. The persistent excitation could possibly be accomplished by the operator's movements, but we ensure excitation by explicitly superimposing high-frequency vibrations.
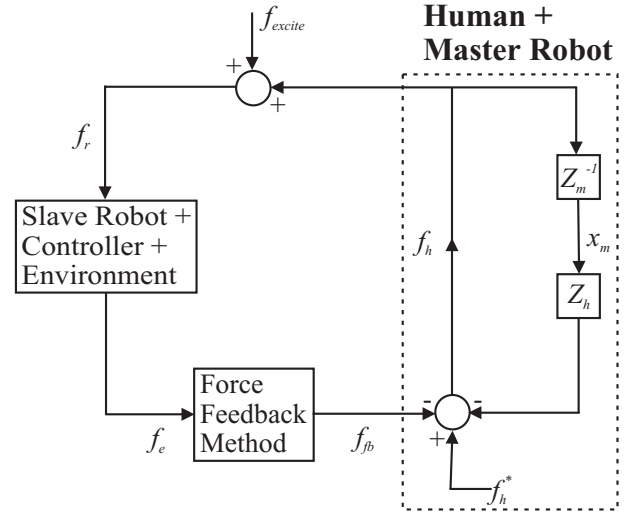
2.1 System Architecture

Bilateral telemanipulation systems may have two-channel or four-channel controllers. Examples of two-channel control architectures are direct force feedback [10], position-position [17], force-force [14], and force-position [16] controllers. In contrast, four-channel controllers transmit both force and position information from the master to slave and vice versa [17]. The telemanipulation architecture we present uses a modified two-channel controller.

Figure 1 provides an overview of the salient components of the proposed system required for parameter estimation during telemanipulation. f_h is the force applied by the human operator to the master robot and is measured by the force sensor on the master side. A position sensor measures the location of the master robot end-effector, x_m. f_r represents the reference force (which includes the excitation signal) provided from the master side. f_e is the interaction force between the slave robot end-effector and its environment, as measured by a force sensor located on the slave robot. x_s is the slave robot end-effector position measured by a position sensor. f_{fb} is the force fed back from the slave side to the master robot and subsequently to the operator.

Figure 2 depicts the block diagram of the bilateral telemanipulation system. The elements corresponding to the *human + master robot* and *slave robot + controller + environment* have been grouped together for clarity. The dynamics and control model of the *human + master robot* is represented by the master robot ($Z_m(s)$) and human hand ($Z_h(s)$) impedances, which are given in (1) and (2), respectively.

$$Z_m(s) = M_m s^2 + B_m s + K_m \tag{1}$$

$$Z_h(s) = M_h s^2 + B_h s + K_h \tag{2}$$

In (1) and (2), M_m, B_m, and K_m, and M_h, B_h, and K_h, represent the effective mass, damping, and stiffness of the master robot and human hand, respectively. In Figure 2, the input to the system is an exogenous force, f_h^*, that the operator intends to apply to the master robot [17]. Since Figure 2 represents a closed-loop telemanipulation system, f_h is the summation of f_h^*, f_{fb}, and the force due to the impedance of the human hand. As mentioned earlier, persistent excitation is essential for good parameter estimation [23], and this is represented by f_{excite}. Further, as seen in Figure 2, $f_r = f_h + f_{excite}$.

The *slave robot + controller + environment* control block has been expanded in Figure 3. The complete control architecture for
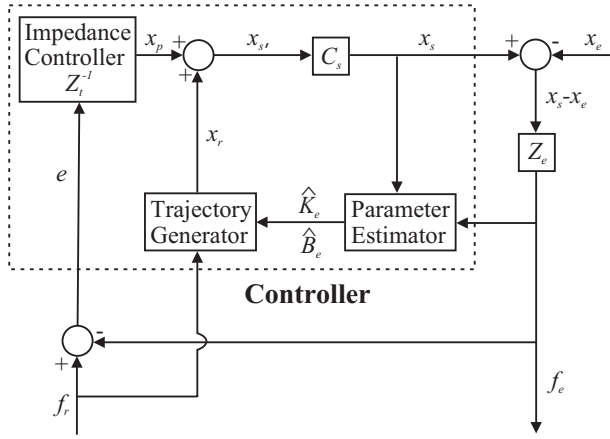
Figure 3: Slave robot + Controller + Environment: Slave robot control system architecture for parameter estimation during bilateral telemanipulation.
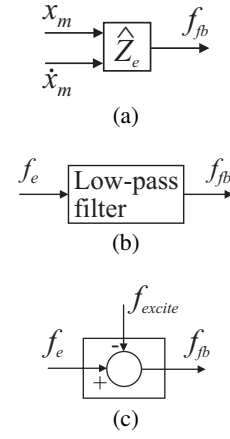

Figure 4: Possible force feedback methods include (a) passing master robot motions through the estimated environment impedance, (b) low-pass filtering the environment contact force, and (c) subtracting the excitation force from the environment contact force.

the slave robot includes the *impedance controller* $Z_t^{-1}(s)$, *trajectory generator*, *parameter estimator*, and position controller C_s. The slave robot is essentially a position-controlled manipulator, and the input to C_s is the commanded position, $x_{s'}$, and the output is the measured position, x_s, of the slave robot end-effector. Further, x_e represents the initial deformation of the environment. Since x_s is the position of the end-effector of the slave robot, which is provided by the slave robot position sensor, the instantaneous deformation of the environment can be computed as $x_s - x_e$. Using the inverse kinematics, joint controllers, and robot dynamics, C_s computes the joint torques required to drive the slave robot.

In Figure 3, x_p is the perturbed trajectory produced by the *impedance controller* and x_r is the reference trajectory generated by the *trajectory generator*. The perturbed trajectory alters the reference trajectory, resulting in the commanded slave robot trajectory, which is tracked by the the slave robot position controller. Further, $\widehat{K}_e$ and $\widehat{B}_e$ are the estimated environment stiffness and damping, respectively, which are computed by the *parameter estimator*. Details and formulation of the *impedance controller*, *trajectory generator*, and *parameter estimator* are provided in Section 3.

The dynamics of the slave robot impedance controller and environment are:

$$Z_t(s) = M_t s^2 + B_t s + K_t \qquad (3)$$

$$Z_e(s) = B_e s + K_e \qquad (4)$$

In (3) and (4), M_t, B_t, and K_t, represent the impedance control gains for the slave robot, and K_e and B_e are the actual stiffness and damping of the soft environment, respectively. For the applications we are considering, the time delays are very small [21]. Hence, the delays caused by the communication channels are not shown in Figures 2 and 3.

2.2 Force Feedback Methods

As mentioned earlier, in Figure 2, f_{excite} represents the persistent excitation required for good parameter estimation [23]. The proposed estimation algorithm is in essence part of a force tracking method, and since the reference force, f_r, is oscillatory, the sensed force between the slave robot end-effector and its environment is also oscillatory. Thus, it is practical to employ a vibration cancellation method prior to feeding back the contact force, f_e, to the human operator. This is represented by the *force feedback method* block in Figure 2.

We consider three force feedback methods, which are depicted in Figure 4 and described as follows:

(a) In Figure 4(a), f_{fb} is based on the position and velocity of the master robot end-effector and the estimated environment parameters:

$$F_{fb}(s) = \widehat{Z}_e(s) X_m(s), \qquad (5)$$

where $\widehat{Z}_e(s)$ represents the estimated environment impedance and $X_m(s)$ is the Laplace transform of the master robot end-effector motions. If good estimation of the environment parameters is achieved, then the operator would be able to feel the environment appropriately. As the user-applied force is constant, $X_m(s)$ is devoid of excitation signals, and thus, $F_{fb}(s)$ is not oscillatory.

(b) In Figure 4(b), f_e is filtered to cancel out the high frequency vibrations. $5 - 10$ Hz is the maximum frequency beyond which the human finger cannot easily apply purposeful force or position commands [22]. So by adding a low-pass filter, the high frequencies (greater than 5 Hz) can be removed before sending them to the operator to ensure a "better feel" of the environment.

(c) As f_{excite} is provided by software, it is a known quantity. Thus, in Figure 4(c), the persistent excitation is explicitly subtracted from the contact force before being fed back to the operator.

The performance of the force feedback methods described in this section in conjunction with the complete bilateral telemanipulation system are examined by software simulations in Section 4.

3 ENVIRONMENT PARAMETER ESTIMATION

In Section 2.1 an overview of the proposed bilateral telemanipulation system involving environment parameter estimation was presented. This section discusses in detail the adaptation law used for environment parameter estimation. As mentioned previously, the slave robot is considered to be position controlled, and the *impedance controller*, *trajectory generator*, and *parameter estimator* are provided as outer control loops. The estimation algorithm is based on force tracking; the goal is to have the contact force between the slave robot end-effector and its environment track the
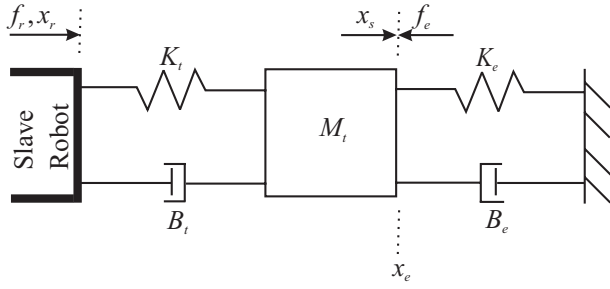
303

Figure 5: Model of the slave robot impedance controller and soft environment.

reference force. To achieve good force control, the position controller has to be accurate. In the method presented, force tracking is achieved by impedance control and an indirect adaptive control strategy for parameter estimation, introduced by Seraji, et al. [20].

3.1 Force Tracking

Impedance control aims to control the position and force by adjusting the mechanical impedance of the end-effector to external forces [12]. The external forces are generated due to contact between the slave robot end-effector and its environment. For the purposes of this study, we consider position-based impedance control. For clarity, we consider the master and slave robots as one degree-of-freedom linear time-invariant systems. The formulation presented can be extended to telerobotic systems with more than one degree of freedom. Figure 5 shows the basic components of the slave robot under impedance control. In general, the impedance controller is chosen as a linear second-order system, where M_t, B_t, and K_t represent the controller gains [20]. Alternatively, M_t, B_t, and K_t could be interpreted as the target mass, damping, and stiffness of the impedance controller, respectively [8]. In Figure 5, the slave robot is assumed to be probing a soft environment via a single point contact.

The variables used in Figure 5 have been defined previously in Section 2.1. As mentioned earlier, x_e is the initial deformation of the environment, so $\dot{x}_e = 0$ and is thus not included in the derivation presented. The force tracking error in terms of the user-applied reference force (including persistent excitations) and the sensed contact force is given as

$$e = f_r - f_e. \tag{6}$$

The impedance controller equation for the slave robot is given by the error dynamics of a second-order system as

$$
\begin{aligned}
e = {} & M_t \left(\ddot{x}_{s'} - \ddot{x}_r \right) + B_t \left(\dot{x}_{s'} - \dot{x}_r \right) \\
& + K_t \left(x_{s'} - x_r \right),
\end{aligned} \tag{7}
$$

where x_r and $x_{s'}$ are the reference and commanded positions of the slave robot end-effector, respectively. Also, the perturbed slave position is given by, $x_p = x_{s'} - x_r$. When the slave robot is not in contact with the environment, $f_e = f_r = 0$ and hence, $x_p = 0$. While the slave robot end-effector probes the environment, the force sensor measures f_e, resulting in perturbation of the reference trajectory. Thus, (7) is rewritten as

$$e = M_t \ddot{x}_p + B_t \dot{x}_p + K_t x_p, \tag{8}$$

which is analogous to a mass-spring-damper system, shown in Figure 5. The perturbed trajectory is used to modify the reference trajectory to generate the commanded slave robot trajectory $(x_{s'} = x_p + x_r)$, which is tracked by slave robot position controller (C_s), as shown in Figure 3. Further, for good slave robot position

control, $x_{s'} \approx x_s$, which implies $x_s = x_p + x_r$. Taking the Laplace transform of (8) and using (4) results in

$$E(s) = Z_t(s) X_p(s). \tag{9}$$

The contact force depends on the actual nonlinear environment stiffness and damping, and can be expressed as

$$f_e = K_e (x_s - x_e) + B_e \dot{x}_s. \tag{10}$$

The mass of the environment is ignored in (10), since for medical robotics applications the environment tends to be quasi-static. Using (6), (10), and $x_s = x_p + x_r$, the error can be rewritten as

$$
\begin{aligned}
e = {} & f_r + K_e (x_e - x_r) - B_e \dot{x}_r - K_e x_p \\
& - B_e \dot{x}_p.
\end{aligned} \tag{11}
$$

Taking the Laplace transform of (11), and using (4) and (9) results in

$$E(s) = \frac{Z_t(s) \left[F_r(s) + Z_e(s) \left(X_e(s) - X_r(s) \right) \right]}{Z_t(s) + Z_e(s)}. \tag{12}$$

Thus, the steady-state force tracking error (e_{ss}) is obtained as

$$e_{ss} = \frac{K_t}{K_t + K_e} \left(f_r + K_e x_e - K_e x_r \right). \tag{13}$$

Further, $e_{ss} \to 0$ as

$$x_r = \frac{f_r}{K_e} + x_e, \tag{14}$$

and $E(s) \to 0$ as

$$\dot{x}_r = \frac{f_r + K_e (x_e - x_r)}{B_e}. \tag{15}$$

Also, substitution of (14) in (15) results in

$$\dot{x}_r = 0. \tag{16}$$

Thus, in order to have perfect force tracking, the slave robot end-effector must follow the reference position and velocity as defined in (14) and (16). In practice, we believe that reasonable environment parameter estimates can be achieved with good force tracking.

3.2 Indirect Adaptive Control

As seen in (14) and (15), accurate knowledge of the environment parameters is necessary for good force tracking. The indirect adaptive control strategy aims to adaptively compute the estimated environment stiffness $(\widehat{K}_e)$ and damping $(\widehat{B}_e)$ online during telemanipulation. The estimated parameters are then used to compute the reference trajectory. Hence, (14) and (16) are rewritten in terms of estimated environment parameters as:

$$x_r = \frac{f_r}{\widehat{K}_e} + x_e. \tag{17}$$

$$\dot{x}_r = 0. \tag{18}$$

The *trajectory generator*, shown in Figure 3, is described by (17) and (18).

In order to develop the indirect adaptive control method for estimating environment parameters used in (17) and (18), consider the estimated contact force:

$$\widehat{f}_e = \widehat{K}_e (x_s - x_e) + \widehat{B}_e \dot{x}_s. \tag{19}$$

Subtracting (10) from (19) results in

$$
\begin{aligned}
\widehat{f}_e - f_e &= \left(\widehat{K}_e - K_e \right)(x_s - x_e) \\
&+ \left(\widehat{B}_e - B_e \right) \dot{x}_s.
\end{aligned}
\tag{20}
$$

Defining $\tilde{f}_e = \widehat{f}_e - f_e$, (20) can be rewritten as

$$
\tilde{f}_e = \phi^T \tilde{\theta},
\tag{21}
$$

where

$$
\phi = \left[\begin{array}{c} x_s - x_e \\ \dot{x}_s \end{array} \right] \quad \text{and} \quad \tilde{\theta} = \left[\begin{array}{c} \widehat{K}_e - K_e \\ \widehat{B}_e - B_e \end{array} \right].
\tag{22}
$$

Estimated parameters should be updated so that the predicted force error ($\tilde{f}_e$) is reduced. In order to achieve this, we use a Lyapunov-based approach [20]. Consider the Lyapunov function candidate

$$
V = \tilde{\theta}^T \Gamma \tilde{\theta},
\tag{23}
$$

where Γ is a positive definite and symmetric gain matrix. For successful parameter estimation, the estimated parameters, $\widehat{\theta} = [\widehat{K}_e \quad \widehat{B}_e]^T$ must be updated in the opposite direction of the gradient of the squared prediction error with respect to the estimated parameters [23], which results in

$$
\dot{\widehat{\theta}} = -\Gamma^{-1} \frac{\partial}{\partial \widehat{\theta}} \left(\tilde{f}_e^T \tilde{f}_e \right).
\tag{24}
$$

Using (21) and (24) results in the following parameter adaptation law [8],

$$
\dot{\tilde{\theta}} = -\Gamma^{-1} \phi \tilde{f}_e.
\tag{25}
$$

From (23) and using (25), the time derivative of the Lyapunov function is computed as

$$
\begin{aligned}
\dot{V} &= 2\tilde{\theta}^T \Gamma \dot{\tilde{\theta}} \\
&= -2\tilde{\theta}^T \phi \phi^T \tilde{\theta} \\
&< 0.
\end{aligned}
\tag{26}
$$

Further, from (23) and (26), we infer that if $\tilde{\theta}$ is adjusted according to parameter estimation law given in (25), then $\tilde{\theta} \to 0$ as $t \to \infty$ i.e. $(\widehat{K}_e, \widehat{B}_e) \to (K_e, B_e)$ [20]. (25) represents the *parameter estimator*, shown in Figure 3. Thus, we have demonstrated that if the slave robot end-effector follows the prescribed reference trajectory, then force tracking is ensured by the impedance controller and accurate estimation of environment parameters is obtained.

4 SIMULATION RESULTS AND DISCUSSION

Numerical simulations were performed to evaluate the proposed method for simultaneous bilateral telemanipulation and environment parameter estimation. The simulations were based on the system presented in Figure 2. The system parameters for the human hand, master robot, and impedance controller used in the simulation studies are provided in Table 1.

In the simulation, the slave robot was commanded to make contact with the soft environment, after which f_h^* was applied as a constant force of 15 N to the master robot. f_{excite} was provided as $4.5\sin(15t)$ N. The gain matrix (Γ) for the parameter adaptation law given in (25) was

$$
\Gamma = \left[\begin{array}{cc} 1500 & 0 \\ 0 & 500 \end{array} \right].
\tag{27}
$$

|		
Human hand (Z_h)	M_h	2.0 kg
	B_h	5.0 kg/s
	K_h	100.0 N/m
Master robot (Z_m)	M_m	2.5 kg
	B_m	50.0 kg/s
	K_m	250.0 N/m
Impedance controller (Z_t)	M_t	5.0 kg
	B_t	450.0 kg/s
	K_t	800.0 N/m
Position controlled slave robot	C_s	1.0

Table 1: Values of system parameters used in numerical simulations.

For the system parameter and f_h^* values chosen, f_{excite} and Γ were selected manually in order to produce stable and accurate estimation of the environment parameters.

Simulations of the system for the three force feedback methods described in Section 2.2 were performed. The schemes used to generate the feedback force were: (1) using the estimated environment impedance, (2) low-pass filtering the environment contact force, and (3) explicitly subtracting the excitation force from the environment contact force. Further, for the purposes of comparison, we also consider feeding back the "measured" contact force without modification.

Figure 6 shows the performance of the environment estimation for the four force feedback methods described above. The solid lines represent the actual nonlinear environment stiffness and damping, and the dashed lines represent the estimation. The stiffness and damping of the soft environment varies nonlinearly with the deformation of the environment from 175 N/m to 230 N/m and 75 kg/s to 100 kg/s, respectively. In the simulations, initial conditions for the environment stiffness and damping estimates were set as 150 N/m and 65 kg/s, respectively. Also, the estimator is active only when the slave robot comes in contact with the environment and reset laws are used to ensure that the estimates do not go to zero. As seen in Figure 6, the indirect adaptive algorithm was able to stably predict the nonlinear environment stiffness and damping for all force feedback methods. The convergence time for the damping estimate varied significantly, depending on the force feedback method. Also, persistent excitation in the reference force was only required for correct estimation and convergence of environment damping, not for stiffness. In order to compare the different force feedback methods, the system inputs and gains were the same for all the simulation cases considered. Thus, better environment damping estimates could be obtained for each method with a different choice of controller gains.

Figure 7 shows the force fed back to the operator for each of the force feedback methods mentioned previously. Figure 7(b), which uses the estimated environment parameters to generate the force feedback, shows the best results in terms of reducing the oscillatory behavior of f_e, and would likely create the most realistic environment sensations for the operator. As mentioned earlier, $5 - 10$ Hz is the maximum frequency range beyond which the human finger cannot apply meaningful position or force commands [22]. So for Figure 7(c), a low-pass filter with cutoff frequency of 2 Hz was applied to remove the high-frequency oscillations from the environment contact force. For the purposes of this simulation study, a 2 Hz low-pass filter was used instead of a $5 - 10$ Hz low-pass filter because the frequency of the excitation signals was not greater than 5 Hz. Using persistent excitation of higher frequency did not produce better results for environment parameter estimation, and in some applications higher frequency excitation might not be advisable. Nonetheless, using low-pass filters to ensure a "better feel" of the environment is still a valid option. Since there is a phase difference between f_r and f_e, direct subtraction of f_{excite} from f_e did not
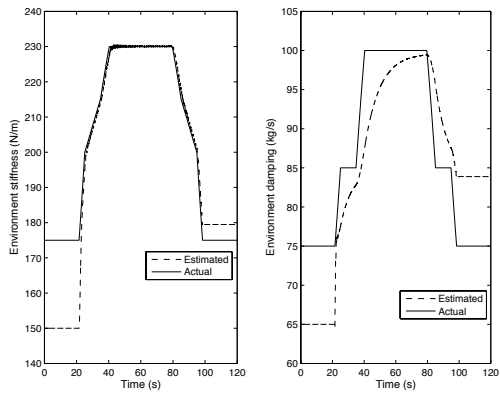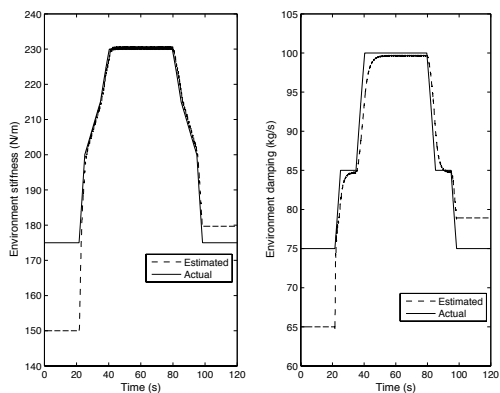
(a) $f_{fb} = f_e$
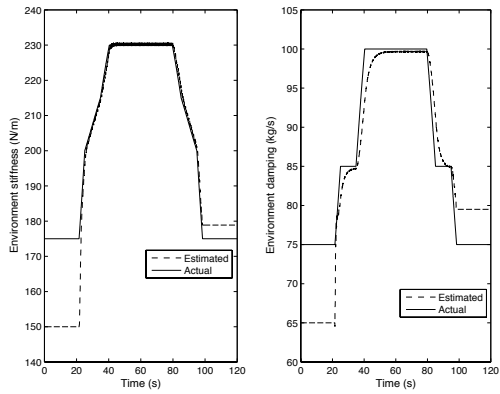
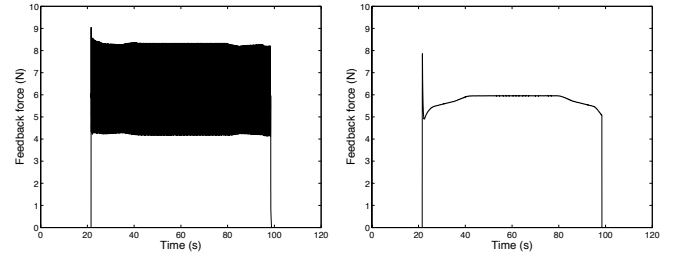
(b) $F_{fb}(s) = \widehat{Z}_e(s) X_m(s)$
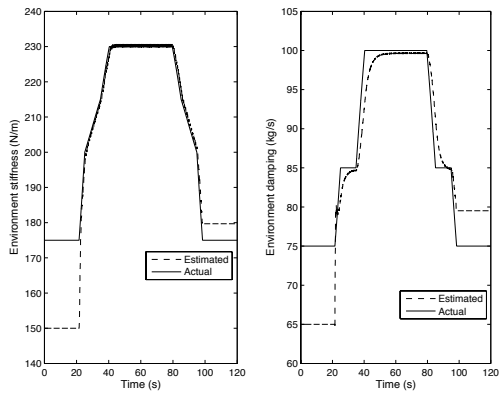
(c) $f_{fb} = \text{Low-pass filter}(f_e)$

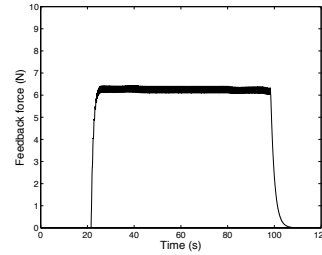

(d) $f_{fb} = f_e - f_{excite}$

Figure 6: Estimated versus actual environment parameters for various force feedback cases during bilateral telemanipulation.

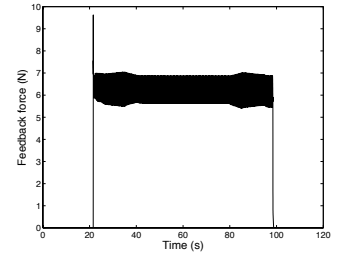reduce the oscillations substantially, as seen in Figure 7(d).

(a) $f_{fb} = f_e$

(b) $F_{fb}(s) = \widehat{Z}_e(s) X_m(s)$

(c) $f_{fb} = \text{Low-pass filter}(f_e)$

(d) $f_{fb} = f_e - f_{excite}$

Figure 7: Feedback force during bilateral telemanipulation

5   CONCLUSION

We presented a bilateral telemanipulator system that used an indirect adaptive control algorithm to estimate soft environment parameters. The scheme was based on achieving force tracking between the reference (user-applied force superimposed with excitations) and environment contact forces. This was done using an online trajectory generator and an indirect adaptation law. The slave robot was a position-controlled manipulator and the estimator control architecture was provided as an outer control loop. This non-intrusive approach for parameter estimation enabled straightforward implementation of control algorithms. Simulation studies showed that it was possible to get accurate and stable estimates for nonlinear environment properties.

Persistent excitation of the environment was required for robustness of the parameter estimator. Since our intended application is surgical robotics, the excitation signals are of small amplitude in order to prevent unwanted tissue motion during robot manipulation. Further, various methods were explored to eliminate the effects of persistent excitation in the force fed back to the human operator, so as to make the parameter estimation process seamless and transparent to the user. It was concluded that using the estimated environment impedance produces the least oscillatory force feedback. Hence, this would give the most realistic feel of environment to the operator during parameter estimation.

In future work, we will implement and test the environment parameter estimation algorithm first on a set of one degree-of-freedom haptic devices equipped with force and position sensors during telemanipulation of a phantom soft tissue environment. Further, we will obtain more complex environment models using telemanipulation systems with more degrees of freedom, such as the da Vinci Surgical System (Intuitive Surgical, Inc., Sunnyvale, CA). Efforts will also be made to theoretically quantify the stability of the proposed telemanipulation system. Sensitivity studies will be done in order to evaluate the effects of force sensor noise, choice of adaptation law gains, and larger variation in environment stiffness and

damping values on the environment property estimation and force feedback to the human. We will also explore variations of the proposed algorithm that eliminate the use of force sensors. In the long-term, we would like to explore the online development of large-scale virtual tissue models based on estimated soft tissue properties.

REFERENCES

[1] I. Brouwer, J. Ustin, L. Bentley, A. Sherman, N. Dhruv, and F. Tendick. Measuring in vivo animal soft tissue properties for haptic modeling in surgical simulation. *Medicine Meets Virtual Reality*, pages 69–74, January 2001.

[2] M. B. Colton and J. M. Hollerbach. Identification of nonlinear passive devices for haptic simulations. In *First Joint Eurohaptics Conf. and Symposium on Haptic Interfaces for Virtual Environment and Teleoperator Systems, World Haptics Conf. (WHC)*, pages 363–368, Pisa, Italy, March 2005.

[3] S. Cotin, H. Delingette, and N. Ayache. A hybrid elastic model for real-time cutting, deformations, and force feedback for surgery training and simulation. *Visual Computer*, 16(8):437–452, November 2000.

[4] S. P. DiMaio and S. E. Salcudean. Needle insertion modeling and simulation. *IEEE Trans. Robotics and Automation*, 19(5):864–875, October 2003.

[5] N. Diolaiti, C. Melchiorri, and S. Stramigioli. Contact impedance estimation for robotic systems. In *IEEE/RSJ Int'l. Conf. on Intelligent Robots and Systems (IROS)*, volume 3, pages 2538–2543, Sendai, Japan, September 2004.

[6] G. Duchemin, P. Maillet, P. Poignet, E. Dombre, and F. Pierrot. A hybrid position/force control approach for identification of deformation models of skin and underlying tissues. *IEEE Trans. Biomedical Engineering*, 52(2):160–170, February 2005.

[7] P. E. Dupont, P. A. Millman, T. M. Schulteis, and R. D. Howe. Automatic identification of environment haptic properties. *Presence: Teleoperators and Virtual Environments*, 8(4):392–409, August 1999.

[8] D. Erickson, M. Weber, and I. Sharf. Contact stiffness and damping estimation for robotic systems. *Int'l. J. Robotics Research*, 22(1):41–57, January 2003.

[9] G. De Gersem, H. Van Brussel, and J. Vander Sloten. Enhanced haptic sensitivity for soft tissues using teleoperation with shaped impedance reflection. In *World Haptics Conf. (WHC)*, Pisa, Italy, March 2005.

[10] B. Hannaford. Design framework for teleoperators with kinesthetic feedback. *IEEE Trans. Robotics and Automation*, 5(4):426–434, August 1989.

[11] K. Hashtrudi-Zaad and S. E. Salcudean. Adaptive transparent impedance reflecting teleoperation. In *IEEE Int'l. Conf. on Robotics and Automation*, volume 2, pages 1369–1374, Minneapolis, USA, April 1996.

[12] N. Hogan. Impedance control: an approach to manipulation: part i-iii. *ASME J. Dynamic Systems, Measurement, and Control,*, 107(1):1–24, March 1985.

[13] T. Hu and J. P. Desai. Characterization of soft-tissue material properties: large deformation analysis. In *Second Int'l. Symposium on Medical Simulation (ISMS)*, pages 28–37, Cambridge, USA, June 2004.

[14] H. Kazerooni, T.-I. Tsay, and K. Hollerbach. Controller design framework for telerobotic systems. *IEEE Trans. Control Systems Technology*, 1(1):50–62, March 1993.

[15] A. E. Kerdok, S. M. Cotin, M. P. Ottensmeyer, A. M. Galea, R. D. Howe, and S. L. Dawson. Truth cube: establishing physical standards for soft tissue simulation. *Medical Image Analysis*, 7(3):283–291, January 2003.

[16] H. Kobayashi and H. Nakamura. A scaled teleoperation. In *IEEE Int'l. Workshop on Robot and Human Communication*, pages 269–274, Tokyo, Japan, September 1992.

[17] D. A. Lawrence. Designing teleoperator architectures for transparency. In *IEEE Int'l. Conf. on Robotics and Automation*, volume 2, pages 1406–1411, Nice, France, May 1992.

[18] M. P. Ottensmeyer, A. E. Kerdok, R. D. Howe, and S. L. Dawson. The effects of testing environment on the viscoelastic properties of soft tissues. In *Second Int'l. Symposium on Medical Simulation (ISMS)*, pages 67–76, Cambridge, USA, June 2004.

[19] J. Park, R. Cortesao, and O. Khatib. Robust and adaptive teleoperation for compliant motion tasks. In *The 11th Int'l. Conf. on Advanced Robotics (ICAR)*, pages 513–519, Coimbra, Portugal, June 2003.

[20] H. Seraji and R. Colbaugh. Force tracking in impedance control. In *IEEE Int'l. Conf. on Robotics and Automation*, volume 2, pages 499–506, Atlanta, USA, May 1993.

[21] A. Sherman, M. C. Cavusoglu, and F. Tendick. Comparison of teleoperator control architectures for palpation task. In *Symposium on Haptic Interfaces for Virtual Environment and Teleoperator Systems (IMECE)*, pages 1261–1268, Orlando, USA, November 2000.

[22] K. B. Shimoga. Survey of perceptual feedback issues in dexterous telemanipulation: Part i. finger force feedback. In *IEEE Annual Virtual Reality Int'l. Symposium*, pages 263–270, Seattle, USA, September 1993.

[23] J.-J. E. Slotine and L. Weiping. *Applied Nonlinear Control*. Prentice-Hall Inc., Englewood Cliffs, NJ, 1991.

[24] V. Vuskovic, M. Kauer, G. Szekely, and M. Reidy. Realistic force feedback for virtual reality based diagnostic surgery simulators. In *IEEE Int'l. Conf. on Robotics and Automation*, volume 2, pages 1592–1598, San Francisco, USA, April 2000.